J|A|C|S
ARTICLES
Published on Web 12/25/2003

Photochemistry and Mobility of Stilbenoid Dendrimers in Their Neat Phases

Matthias Lehmann,*[,†,§] Ingrid Fischbach,[‡] Hans Wolfgang Spiess,[‡] and Herbert Meier[†]

Contribution from the Institut für Organische Chemie, University of Mainz, Duisbergweg 10-14, 55099 Mainz, Germany, and Max Planck Institute for Polymer Research, Ackermannweg 10, 55118 Mainz, Germany

Received June 11, 2003; E-mail: matthias.lehmann@ulb.ac.be

Abstract: Selectively deuterated, dodecyloxy substituted stilbenoid dendrimers of the first and second generation were synthesized by a convergent synthesis, using the Wittig−Horner reaction. The photochemistry and the fluorescence in the different crystalline and liquid crystalline phases were investigated. Molecules deuterated at the α-position of the alkoxy chains were used to study the photoreactions in the neat phases by ^{1}H NMR. Reactions of the double bonds are exclusively observed in the liquid crystal phases. No photoreactions occur in the crystalline state. The mobility of the dendrimers was studied by means of ^{2}H solid-state NMR spectroscopy. The onset of the photochemistry for dendrimer **1** [all-(*E*)-1,3,5-tris[2-(3,4,5-tridodecyloxyphenyl)ethenyl]benzene] corresponds to the increasing mobility at the Cr/LC transition. The first generation dendrimers still show large angle motion, whereas dendrimers of the second generation **2** [all-(*E*)-1,3,5-tris(2-{3,5-bis[2-(3,4,5-tridodecyloxyphenyl)ethenyl]phenyl}ethenyl)benzene] are restricted to librational motions. Photochemical conversion and fluorescence quenching for first and second generation dendrimers **1** and **2** increase with increasing molecular motion and reach a maximum in the isotropic phase.

Introduction

Compounds based on stilbenoid units play an increasing role in materials science. Their interesting photochemical and photophysical properties which can be easily tuned for specific applications make them prone not only for photoresists, imaging and optical switching techniques, and nonlinear optics but also for optoelectronic devices, such as light-emitting diodes, photoconductors, or photovoltaic cells.[1−4] The latter applications are of emerging interest, and the fabrication of cheap, flexible plastic devices is envisaged.

Recently, stilbenoid compounds have been incorporated in a new structural concept, the dendrimers.[5] Stilbenoid dendrimers have been synthesized by various methods,[5−8] with stilbenoid units of different conjugation lengths up to the fifth generation.[6,9] Their photophysical properties have been studied with respect to their ability toward charge transport,[10] light emission,[11] and electron transfer.[12] Attachment of long alkyloxy chains to their periphery not only effects their solubility in conventional organic solvents but also induces liquid crystal phases for the first two generations.[5,6] Irradiation of stilbenoid dendrimers in cyclohexane solution or of spin-coated thin films results in a fast photodegradation of almost all double bonds.[7,13,14] Photoreactions in the mesophases afford a slight decrease of the clearing temperatures for small amounts of photoproducts; prolonged exposure to UV light results in an irreversible formation of an isotropic phase.[7,13] It has been shown that oligomeric and polymeric photoproducts were formed by statistical CC bond formation. This is in contrast to the photochemistry in diluted solutions, where a high proportion of regular dimers (cyclophanes) is produced.[13] From other stilbenoid mesogens, namely the triphenanthro anellated [18] annulenes,[15] a behavior more similar to that of the photochemistry in solution is known: there,

† University of Mainz.
‡ Max Planck Institute for Polymer Research.
§ Current address: Laboratoire de Chimie des Polymères CP206/1, Université Libre de Bruxelles, Boulevard du Triomphe, 1050 Bruxelles, Belgium.

(1) Meier, H. *Angew. Chem., Int. Ed. Engl.* **1992**, *31*, 1399 and references therein.
(2) Salaneck, W. R.; Lundström, I.; Rånby, B. *Conjugated Polymers and related Materials*; Oxford University Press: Oxford, 1993.
(3) Müllen, K.; Wegner, G. *Electronic Materials: The Oligomer Approach*; Wiley-VCH: Weinheim, 1998.
(4) Meier, H.; Stalmach, U.; Fetten, M.; Seus, P.; Lehmann, M.; Schnorpfeil, C. *J. Inf. Rec.* **1998**, *38*, 47.
(5) Meier, H.; Lehmann, M. *Angew. Chem., Int. Ed.* **1998**, *37*, 643.
(6) Meier, H.; Lehmann, M.; U. Kolb, *Chem.−Eur. J.* **2000**, *6*, 2462−2469.
(7) Meier, H.; Lehmann, M. In *Encyclopedia of Nanoscience and Nanotechnology*; Nalwa, H. S., Ed.; American Scientific Publisher: Stevonson Ranch, CA 2003; Vol. X, pp 1−12.
(8) Deb, S. K.; Maddux, T. M.; Yu, L. *J. Am. Chem. Soc.* **1997**, *119*, 9097.
(9) Lehmann, M.; Schartel, B.; Hennecke, M.; Meier, H. *Tetrahedron* **1999**, *55*, 13377.
(10) Lupton, J. M.; Samuel, I. D. W.; Beavington, R.; Burn, P. L.; Bässler, H. *Adv. Mater.* **2001**, *13*, 258.
(11) Pillow, J. N. G.; Halim, M.; Lupton, J. M.; Burn, P. L.; Samuel, I. D. W. *Macromolecules* **1999**, *32*, 5985.
(12) Guldi, D. M.; Swartz, A.; Luo, C.; Gómez, R.; Segura, J. L.; Martín, N. *J. Am. Chem. Soc.* **2002**, *124*, 10875.
(13) Petermann, R.; Schnorpfeil, C.; Lehmann, M.; Fetten, M.; Meier, H. *J. Inf. Rec.* **2000**, *25*, 259−264.
(14) Meier, H.; Lehmann, M.; Schnorpfeil, Ch.; Fetten, M. *Mol. Cryst. Liq. Cryst.* **2000**, *352*, 85−92.
(15) Müller, K.; Meier, H.; Bouas-Laurent, H.; Desvergne, J. P. *J. Org. Chem.* **1996**, *61*, 5474−5480.

10.1021/ja0366179 CCC: $27.50

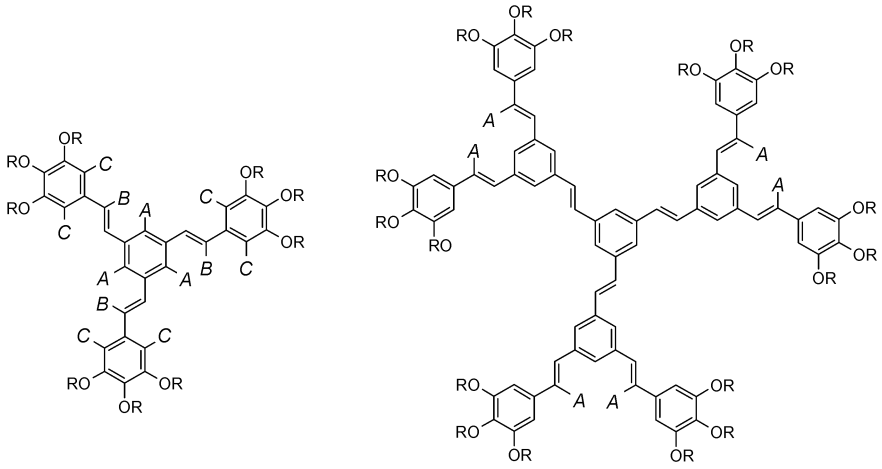

1a *A-C* = ^{1}H, R = $C_{12}H_{25}$ **2a** *A* = ^{1}H, R = $C_{12}H_{25}$

1b *A* = ^{2}H, *B, C* = ^{1}H, R = $C_{12}H_{25}$ **2b** *A* = ^{2}H, R = $C_{12}H_{25}$

1c *B* = ^{2}H, *A, C* = ^{1}H, R = $C_{12}H_{25}$ **2c** *A* = ^{1}H, R = $C^2H_2C_{11}H_{23}$

1d *C* = ^{2}H, *A, B* = ^{1}H, R = $C_{12}H_{25}$

1e *A-C* = ^{1}H, R = $C^2H_2C_{11}H_{23}$

Figure 1. Selective deuterated stilbenoid dendrimers of first and second generation **1** and **2**.

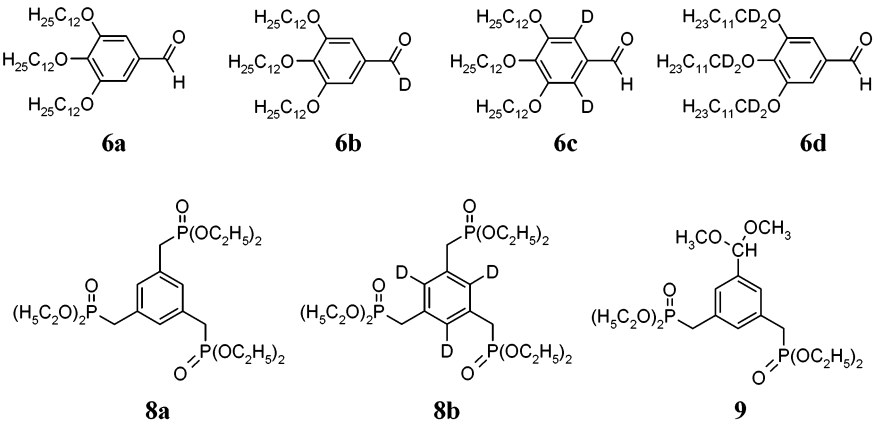

Figure 2. Deuterated building blocks for the synthesis of stilbenoid dendrimers.

the neat mesophase is photochemically inert up to temperatures of around 150 °C where the photodimerization starts, which becomes a quantitative process above 200 °C. Investigations of the mesogenic stilbenoid dendrimers under polarized light without UV filters typically show a fast degradation of the LC phase, especially in the vicinity of the clearing point. Since the photochemical behavior is crucial for the performance of most of the potential applications of stilbenoid dendrimers, it is essential to gain a deeper understanding of the photochemical and photophysical behavior and the underlying structural and molecular dynamical features. Molecular dynamics can be easily and precisely probed by ^{2}H NMR spectroscopy.[16] For this reason, stilbenoid dendrimers of the first and second generation (**1**, **2**) were selectively deuterated from the center to the periphery (Figure 1). In this study, the results from the temperature-dependent ^{2}H NMR experiments will be related to the photochemistry and photophysics of the stilbenoid dendrimers, which are probed by fluorescence spectra and irradiation experiments on the neat materials.

Synthesis

The synthesis[17] of the deuterated dendrimers **1** and **2** (Figure 1) was carried out in a convergent procedure coupled for the individual generations as previously described for nondeuterated derivatives.[5,6] The preparation was conveniently performed using three initial building blocks: peripheral units **6**, core unit **8**, and branching unit **9** (Figure 2). To gain information on different segment mobilities by ^{2}H solid-state NMR, target compounds **1** and **2** were selectively deuterated at various positions; core, double bonds, peripheral aromatic units, and α-CH_2. The deuteration was achieved by synthesis of cores **8** and aldehydes **6** (Figure 2). The deuterated peripheral units **6b**,**d** were prepared analogously to the nondeuterated compound **6a**[18] (Scheme 1), using deuterated reagents, i.e., 1,1-dideuteriododecylbromide[19]

(16) Schmidt-Rohr, K.; Spiess, H. W. *Multidimensional Solid-state NMR and Polymers;* Academic Press: London, 1994.
(17) Experimental details on synthesis, irradiation, and fluorescence experiments and the spectroscopic investigations are collected in the Supporting Information.
(18) Kosteyn, F.; Meier, H.; Zerban, G. *Chem. Ber.* **1992**, *125*, 893−897.
(19) Warner, R. M.; Leich, L. C. *J. Labeled Compd.* **1965**, *1*, 42−53.

Scheme 1. Synthesis of Selectively Deuterated Aldehydes **6** and **10**[a]

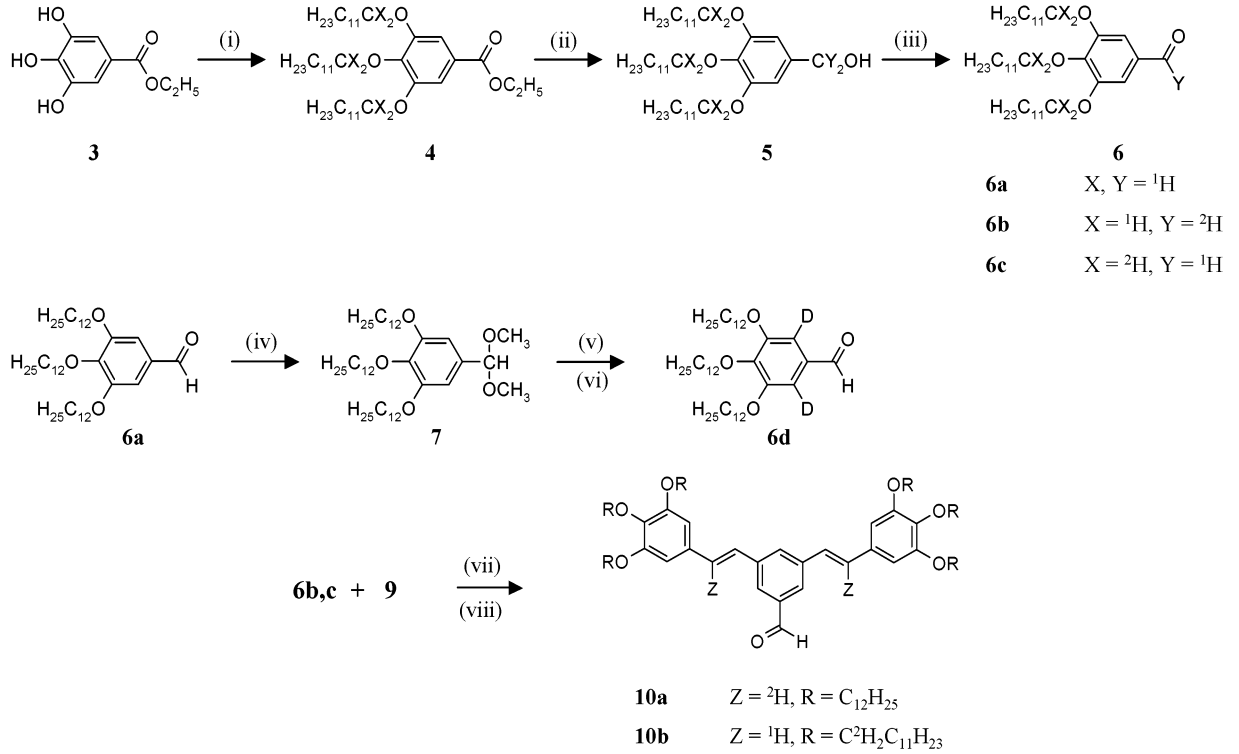

[a] (i) $H_{23}C_{11}CX_2Br$, K_2CO, acetone, reflux; (ii) $LiAlY_4$, $(H_5C_2)_2O$; (iii) DDQ, dioxane, rt; (iv) CH_3OH, $HC(OCH_3)_3$, Dowex 50W-X8; (v) TMEDA, BuLi, Et_2O, D_2O; (vi) HCl, $CHCl_3$; (vii) Ko-*t*-C_4H_9, THF; (viii) HCl, $CHCl_3$.

in the first reaction step toward **6d** and $LiAlD_4$ for the reduction of the ethyl ester (step 2) to obtain **6b**. The deuteration of the aromatic ring in **6c** was achieved via a 2-fold lithiation of a dimethylacetale-protected aldehyde **7**;[20] subsequent quenching with D_2O and cleavage of the acetale gave **6c**, deuterated by 95% at the 2,6-positions. Deuterium at the center of the molecule was introduced by using trideuterio trisphosphonate **8b** as the core unit. It was prepared according to literature procedures[6,21,22] starting from deuterated mesitylene.[23] The deuterated first generation dendrimers **1a**−**d** could then be obtained by a 3-fold Wittig−Horner reaction of the aldehydes **6** with the trisphosphonates **8**. For the preparation of second generation dendrimers **2**, a 2-fold Wittig−Horner reaction of **6** with **9** and subsequent cleavage of the acetale were carried out to provide the dendrons **10a**,**b** (Scheme 1). The latter were coupled to the trisphosphonate **8a** in order to obtain the second generation dendrimers **2b**,**c**. All synthesized deuterated dendrimers were exhaustively purified by column chromatography and succeeding reprecipitation from THF using methanol. By this method, small amounts of photoproducts could be removed, which are formed during synthesis and have a dominant influence on the phase transition characteristics.[7]

Results and Discussion

Thermal Behavior of Neat Samples. The thermotropic behavior of the dendrimers was analyzed by differential scanning calorimetry (DSC) measurements. Phase transitions are in accordance with the data previously published for the nondeuterated samples.[6] Data for the second heating and first cooling curve are collected in Table 1. For all derivatives of series **1**, the second heating curves show two transitions between crystalline phases assigned as Cr_{1-3}, one transition between the Cr_3 phase and the Col_{hd} phase (37.4 ± 0.5 °C/38.0 ± 14.7 kJ/mol) and one transition from the liquid crystal phase to the isotropic phase (74.4 ± 1.0 °C/10.0 ± 0.3 kJ/mol). In the cooling process, only two transitions are observed, one with a small hysteresis at 72.7 ± 1.8 °C (−9.2 ± 0.3 kJ/mol) which corresponds to the conversion from the isotropic to the LC phase and one with a large hysteresis at 8.9 ± 1.3 °C (−61.4 ± 2.6 kJ/mol). The latter is related to the crystallization of the LC phase to the low-temperature crystal phase Cr_1. The transition

Table 1. DSC Results for Stilbenoid Dendrimers **1** and **2** at a Heating Rate of 10° C/min

dendrimer		phase transitions (onset [°C]/Δ*H* [kJ/mol]) heating rate 10 °C/min
1a	heating	Cr_1 13.2/49.4 Cr_2 18.8/−21.0 Cr_3 37.9/39.1 Col_{hd} 75.3/10.1 I
	cooling	I 74.0/−9.5 Col_{hd} 8.2/−60.1 Cr_1
1b	heating	Cr_1 14.2/59.2 Cr_2 18.9/−11.7 Cr_3 36.7/13.5 Col_{hd} 75.4/9.6 I
	cooling	I 74.9/−9.1 Col_{hd} 11.0/−59.3 Cr_1
1c	heating	Cr_1 12.8/42.6 Cr_2 18.0/−21.8 Cr_3 37.7/43.4 Col_{hd} 74.6/10.3 I
	cooling	I 72.4/−9.3 Col_{hd} 8.2/−59.5 Cr_1
1d	heating	Cr_1 12.0/24.4 Cr_2 17.2/−24.0 Cr_3 37.3/52.8 Col_{hd} 73.1/9.8 I
	cooling	I 70.3/−8.8 Col_{hd} 9.2/−65.2 Cr_1
1e	heating	Cr_1 12.2/52.2 Cr_2 18.2/−22.2 Cr_3 37.3/41.3 Col_{hd} 73.7/10.2 I
	cooling	I 71.7/−9.2 Col_{hd} 7.9/−63.0 Cr_1
2a	heating	Cr 11.0/59 Col_{hd} 32.0/4 Col_{ob} 99/17 I
	cooling	I 91/−17 Col_{ob} 5/−48 Cr
2b	heating	Cr 4.1/59.1 Col_{hd} 29.7/20.4 Col_{ob} 98.3/19.6 I
	cooling	I 94.8/−18.6 Col_{ob} 8.7/−47.4 Cr
2c	heating	Cr 2.2/40.9 Col_{hd} 27.5/11.1 Col_{ob} 94.6/11.3 I
	cooling	I 91.2/−11.0 Col_{ob} 5.2/−38.2 Cr

(20) Plaumann, H. P.; Keay, B. A.; Rodrigo, R. *Tetrahedron Lett.* **1979**, *51*, 4921−4924.
(21) Vögtle, F.; Lichtenthaler, R. G.; Zuber, M. *Chem. Ber.* **1973**, *106*, 717−718.
(22) Malkes, L. Y.; Kovalenko, N. P. *Zh. Org. Khim.* **1966**, *2*, 297; *Chem. Abstr.* **1966**, *65*, 2188a.
(23) Andreou, A. D.; Bulbulian, R. V.; Gore, P. H.; Morris, D. F. C.; Short, E. L. *J. Chem. Soc., Perkin Trans. II* **1981**, 830−837.

enthalpy equals the sum of the three transitions detected during the heating cycle.

Dendrimers **2** show a similar behavior. In the heating curves, three transitions Cr/Col_{hd} (5.8 ± 4.6 °C/53.0 ± 10.5 kJ/mol), Col_{hd}/Col_{ob} (29.7 ± 2.3 °C/11.8 ± 8.2 kJ/mol) and Col_{ob}/I (97.3 ± 2.4 °C/16.0 ± 4.2 kJ/mol) take place. Thereby, transitions between the hexagonal phase and the oblique phase appear very broad and can be supercooled; consequently, the cooling curves exhibit only two transitions at 92.3 ± 2.1 °C (−15.5 ± 4.0 kJ/mol) and 6.3 ± 2.1 °C (−44.5 ± 5.5 kJ/mol). Interestingly, the phase sequence of these dendritic mesogens is inverted (Col_{hd} at lower temperatures than Col_{ob}) compared to other discotic molecules forming columnar phases.[24] This may be attributed to the presence of several conformation isomers, whose distribution changes with temperature and, thus, might lead to the observed distortion of the hexagonal phase at elevated temperatures.

NMR Background. In solid-state ^{2}H NMR, the NMR frequency ω_Q (in the rotating frame) depends on the orientation of the external static magnetic field B_0 with respect to the principal axes system of the electric-field gradient (EFG) tensor.[16] ω_Q is described by the following equation:

$$\omega_Q = \pm\frac{\delta}{2}(3\cos^2\theta - 1 - \eta\sin^2\theta\cos 2\varphi) \qquad (1)$$

where θ and φ are the polar coordinates of the magnetic field in the principal axes system of the EFG tensor. The anisotropy parameter δ of the quadrupolar interaction is on the order of $2\pi \times 125$ kHz for C−D deuterons. η is the asymmetry parameter of the electric field gradient (EFG) tensor and is usually negligibly small for C−D bonds. Since the deuteron is a spin-1 nucleus, two transitions are allowed between the corresponding three energy levels, which is reflected in the two signs in eq 1. One-dimensional ^{2}H NMR spectra are usually recorded by applying the solid-echo pulse sequence, which consists of two $\pi/2$ pulses separated by an echo delay t_p and shifted in phase by $\pi/2$. The solid-echo sequence leads to the formation of an echo at $t = 2t_p$. In absence of molecular motions, the line shape of the 1D spectrum is independent of the length of the applied echo delay t_P. In this static case, the signal of isotropic media results from summing over all values of θ and φ and is commonly referred to as the Pake spectrum (assuming an axially symmetric EFG tensor ($\eta = 0$)), which features two singularities with a separation δ ($\theta = 90°$) and feet with a total width of 2δ ($\theta = 0$).

In contrast, if molecular reorientations take place during the pulse sequence, a time-dependent signal $\omega_Q(t)$ results.[25] In this case, the line shape of the 1D spectra is very sensitive to both the kind of motion and the interpulse delay t_P. Therefore, detailed information about the mechanism of molecular reorientation can be extracted by carrying out a line shape analysis.

^{2}H NMR Investigations. From various discotic systems, it is well-known that different segments in the molecule might exhibit large differences in the mobility.[26,27] To distinguish molecular motions and different segmental motions, **1** was selectively deuterated at various positions as shown in Figure 1. Dendrimer **1b** is deuterated at the central benzene ring; thus, the results obtained for this sample reflect the molecular motion of the whole mesogen. Additional dynamics of the dendrimer arms can subsequently be investigated by analyzing the spectra of the molecules selectively deuterated at the olefinic and the outer aromatic positions, **1c** and **1d**. The sample **1e** deuterated at the α-CH_2 groups of the alkoxy chains finally provides information about the restricted mobility of the side chain in the vicinity of the aromatic core. For the ^{2}H NMR studies of the second generation dendrimer **2**, two different isotopomers were prepared, which are shown in Figure 1. Molecules **2b** and **2c** were selectively deuterated at the second shell of the dendrimer, the outer olefinic positions and the α-methylene units of the side chains, respectively. A deuteration of the outer parts of the molecule was preferred over a deuteration of the core moieties, since the very low overall content of ^{2}H in the case of core deuteration would have presumably led to severe signal-to-noise problems.

A. First Generation Dendrimers 1. In the following section, we focus on the sample selectively deuterated at the central benzene ring, **1b**. The temperature-dependent ^{2}H NMR spectra are presented in Figure 3. At 22 °C **1b** is in its crystalline Cr_3 phase. Hence, no significant mobility of the core of the molecule is expected, and correspondingly, the spectrum of **1b** has a Pake pattern with a quadrupole splitting of 130 kHz, which is the typical splitting constant of a rigid C−D bond. Therefore, the core of the molecule is immobile on the fast time scale ($\leq 10^{-4}$ s). Heating to 67 °C and 72 °C into the liquid crystalline phase leads to spectra with a strongly reduced quadrupolar splitting of 46 kHz. The spectra also exhibit a comparably strong signal at ω_0, which is due to isotropic parts in the sample and will be discussed in detail below. The observed reduction of the quadrupolar splitting is due to the onset of the rotation of the mesogens. It should be noted that for symmetry reasons in the fast motional limit a free rotation cannot be distinguished from three-site (or higher) jumps by means of ^{2}H NMR line shape analysis. Discrete three-site jumps (120°) around the column axis are known from other discotic molecules with C_3 symmetry.[27] In the following, we refer to a rotation around the column axis as the motional process, keeping in mind that as well in-plane 120° jumps might take place. In the case of an ideal rotation around the C_3 symmetry axis of the molecule, a reduction of the quadrupolar splitting by a factor 0.5 to ∼65 kHz is expected. Further reduction of the quadrupolar splitting is due to less well-defined rotational motion. In the case of nonaligned, isotropic samples, the order parameter for the disk rotation can be defined as

$$S = \frac{2\delta_{\text{observed}}}{\delta} \qquad (2)$$

The measured reduction to 46 kHz therefore corresponds to an order parameter of $S = 0.74$. Usually in discotic systems order parameters $S > 0.8$ are observed.[28,29] The reduced order parameter obtained in this system can be explained by the dynamics of the dendritic arms as will be shown later with

(24) Cammidge, A. N.; Bushby, R. J. In *Handbook of Liquid Crystals*; Demus, D., Gray, G. W., Spiess, H.-W., Vill, V., Eds.; VCH: 1998; Vol. 2B, pp 781−798.
(25) Spiess, H. W.; Sillescu, H. *J. Magn. Res.* **1981**, *42*, 381.
(26) Spielberg, N.; Sarkar, M.; Luz, Z.; Poupko, R.; Billards, J.; Zimmermann, H. *Liq. Cryst.* **1993**, *15* (3), 311.
(27) Leisen, J.; Werth, M.; Boeffel, C.; Spiess, H. W. *J. Chem. Phys.* **1992**, *97* (5), 3749.
(28) Goldfarb, D.; Luz, Z. *J. Physique* **1981**, *42*, 1303−1311.
(29) Herwig, P.; Kayser, C. W.; Müllen, K.; Spiess, H. W. *Adv. Mater.* **1996**, *8*, 510−513.

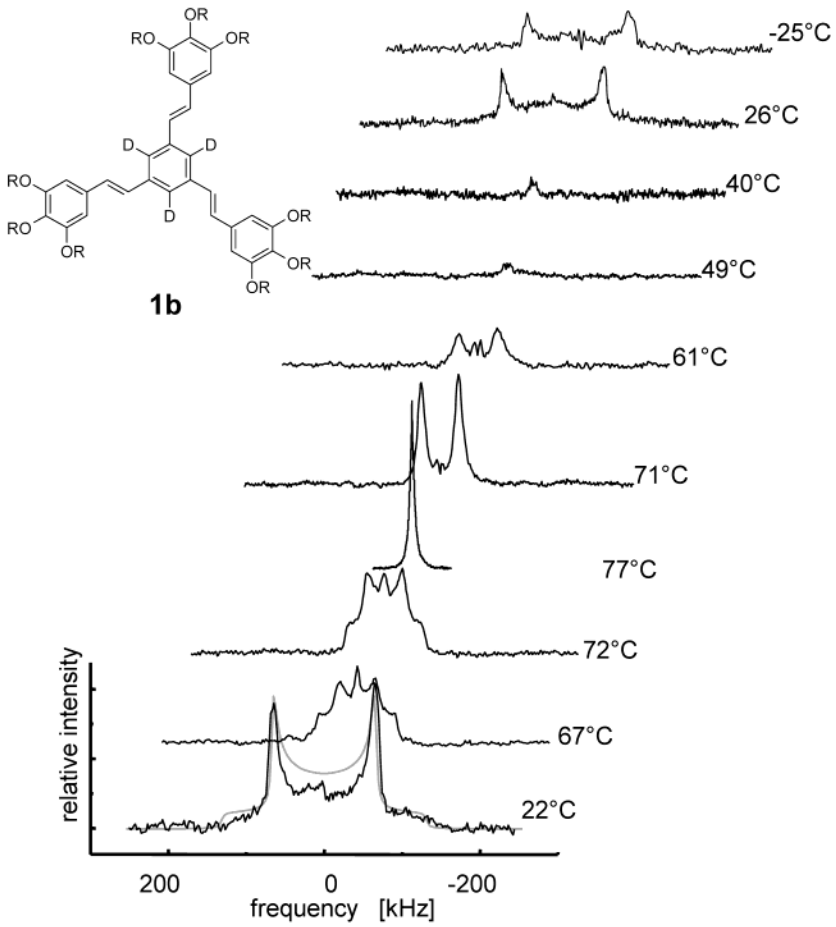

Figure 3. Temperature-dependent ^{2}H NMR spectra of **1b**. The second spectrum (gray) at 22 °C is a simulated Pake pattern with a quadrupole splitting of 130 kHz.

dendrimers **1c** and **1d**. It should be noted that in principle the smaller quadrupolar splitting could originate from a tilt of the molecules with respect to the columnar axis. Assuming ideal order ($S = 1$), the reduced quadrupolar splitting for a tilted arrangement is given by

$$\bar{\delta} = 0.5\delta(3\cos^2\alpha - 1) \qquad (3)$$

where α is the angle between the C−D bond and the rotation axis. For $\alpha = 40.4°$ also, a splitting of 46 kHz would be expected. However, powder X-ray studies reveal a hexagonal columnar disordered phase (Col_{hd}). A tilt of the molecules by 41° would lead to an ecliptical distortion. Such a distortion is usually combined with a loss of symmetry in the column packing in order to get a closest packing,[30] which is not observed in our case. Therefore, we favor the conclusion that the mesophase of the stilbenoid dendrimers is characterized by a rotation of the molecules around the columnar axis with additional out-of-plain motions, which are indicated by the low order parameter.

At 77 °C the material is in its isotropic phase, and only a narrow, intense isotropic signal remains. Cooling the sample slowly down to 71 °C into the liquid crystalline phase leads to a spectrum with two sharp singularities corresponding to a motionally reduced splitting of, again, 48 kHz. The occurrence of two peaks instead of a motionally averaged powder pattern is due to alignment of the aromatic cores and thus of the columns orthogonal with respect to the magnetic field, which is a well-known phenomenon for liquid crystals containing aromatic building blocks.[31] Due to the anisotropy of the magnetic susceptibility of aromatic systems, the potential energy is minimized, when the normal vectors of the aromatic planes are oriented orthogonal to the magnetic field. In the case of aligned samples, determination of the order parameter S from the observed splitting in the ^{2}H NMR spectrum has to take the macroscopic alignment into account. For uniaxial, magnetically aligned samples, the motional order parameter is given by eq 4:

$$S = \frac{2\delta_{\text{observed}}}{\delta(3\cos^2\alpha - 1)(3\cos^2\vartheta - 1)} \qquad (4)$$

where α is the angle between the C−D bond and the rotation axis and ϑ is the angle between the external magnetic field B_0 and the rotation axis. If the rotation axis lies orthogonal to the direction of the magnetic field ($\vartheta = 90°$) and $\alpha = 90°$, which is the case when aromatic mesogens forming an uniaxial hexagonal columnar phase are allowed to minimize their interaction with B_0, an order parameter $S = 0.74$ results, which is identical to the one observed during the heating process. On cooling the sample to lower temperatures, the spectra broaden significantly. At 49 °C the signal almost completely disappears,

(30) Chandrasekhar, S. In *Handbook of Liquid Crystals*; Demus, D., Goodby, J., Gray, G. W., Spiess, H. W., Vill, V., Eds.; Wiley-VCH: Weinheim, 1998; Vol. 2B, pp 749−780.

(31) Bothner-By, A. A. In *Encyclopedia of NMR*; Grant, D. M., Harris, R. K., Eds.; Wiley: Chichester, 1996; Vol. 5.

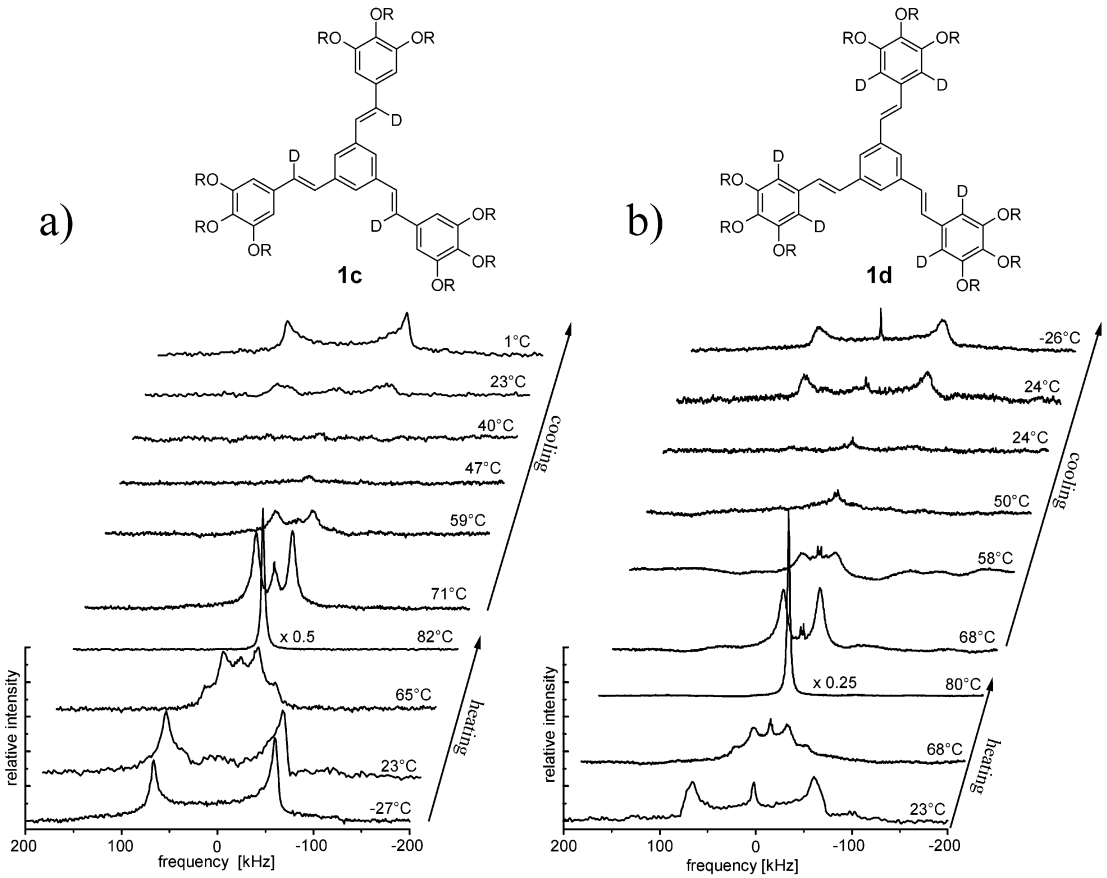

Figure 4. (a) Temperature-dependent ^{2}H NMR spectra of **1c**. The intensity of the spectrum at 82 °C was scaled down by a factor of 0.5. (b) Temperature-dependent ^{2}H NMR spectra of **1d**. The intensity of the spectrum at 82 °C was scaled down by a factor of 0.25. The spectrum at 24 °C was measured first directly and then after annealing for some hours to probe slow crystallization effects.

because of an intermediate motion on the experimental time scale.[25] Cooling further down to 26 °C and annealing leads again to a rigid splitting of 130 kHz, indicating that a crystalline phase has formed. At −25 °C the spectrum exhibits no further change of the quadrupole splitting.

Figure 4 shows the temperature-dependent ^{2}H NMR spectra of the samples deuterated at the olefinic and outer aromatic positions, **1c** (Figure 4a) and **1d** (Figure 4b). Both compounds exhibit the same temperature behavior as **1b**. The rigid quadrupolar splitting of 127 kHz in **1c,d** is only slightly lower than in **1b**. However, in the liquid crystalline phase, the quadrupolar splitting of both compounds is reduced to 38 kHz, which is 10 kHz less than the quadrupolar splitting observed for dendrimer **1b**, deuterated at the central benzene ring. The identical splitting for **1c** and **1d** indicates that both the olefin and the outer aromatic rings are on average tilted out of the plane of the inner benzene ring by the same absolute value of the tilt angle. Indeed as it is obvious from Figure 5, the C−D bonds for both positions form identical angles ± α with the rotation axis, provided the olefinic and the aromatic units lie in the same plane. In this arrangement, the angle α between the C−D bond and the rotation axis is given by

$$\cos \alpha = \cos(90° - \tau) \times \cos 30° \qquad (5)$$

where τ is the torsional angle as depicted in Figure 5. This torsion out of the plane causes the additional reduction of the observed quadrupolar splitting by a factor of 0.81. From eq 3 it follows immediately that this reduction factor equals 0.81 = (3 $\cos^2 \alpha - 1$) and, hence, α is ±39°. This corresponds to a torsional angle $\tau = \pm 26°$. Such a torsion of the dendritic arms out of the inner aromatic planes does not require much energy.[1] From force field simulations of similar systems,[1,32] it is well-known that the inharmonic slope of the potential for the torsion out of the plane is very shallow and increases significantly only at torsional angles above ±30°. The observed torsional angle of ±26° is therefore typical for stilbenoid compounds.[1,7,32] It

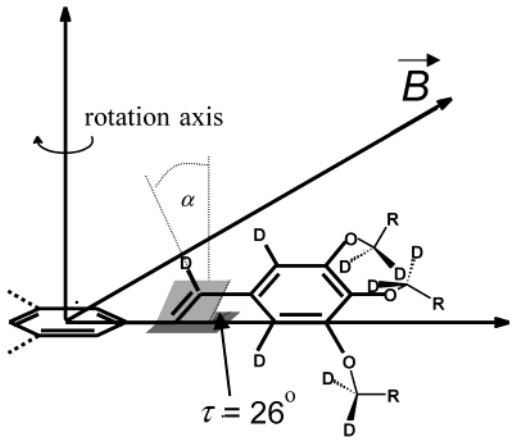

Figure 5. Schematic drawing of the torsional angle (dihedral angle) τ of the dendritic arm of **1** out of the inner aromatic plane and the angle α enclosed between the CD bond and rotational axis.

(32) Karabunarliev, S.; Baumgarten, M.; Tyutyulkov, N.; Müllen, K. *J. Phys. Chem.* **1994**, *46*, 11892−11901.

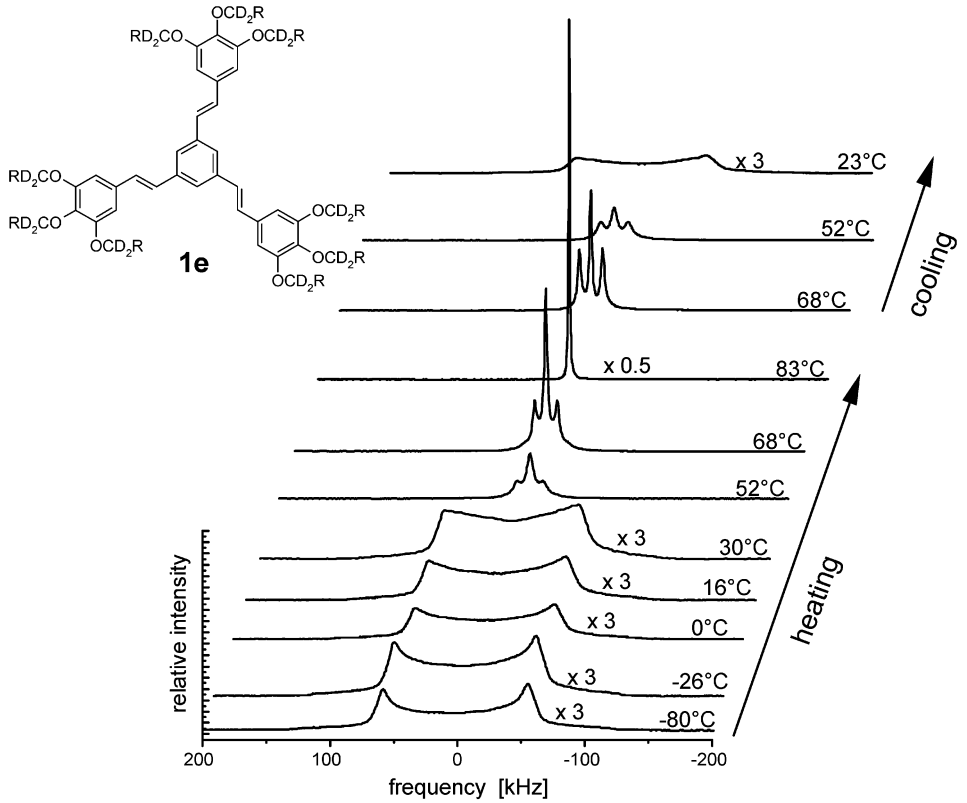

Figure 6. Temperature-dependent ^{2}H NMR spectra of **1e**. The spectra are scaled by the factors indicated in the figure.

should be noted that the line shape of the ^{2}H NMR spectra does not allow for a conclusive distinction as to whether the dendritic arms are in a dynamic average between various conformations or represent stiff segments causing a propeller-like structure of the dendrimer in the mesophase, as it is visualized for dendrimers of third or higher generation.[6] However, the very low activation barriers around the planar minima[1,33] makes the latter case appear improbable, as long as an isolated molecule is considered. Steric constraints in the columnar packing might principally lead to a stiff propeller-like structure as it was observed in polyphenylene dendrimers.[34] In disordered hexagonal columnar phases (Col_{hd}), however, this is unlikely.

In Figure 4b, two spectra of **1d** at 24 °C (cooling) are shown: one measured immediately after reaching 24 °C and the other measured after annealing the sample for 1 h. Clearly, the signal intensity of the annealed sample is much higher, indicating that the mesophase can be supercooled considerably and crystallizes slowly.

In the spectra of **1b**, **1c**, and **1d**, an additional isotropic signal of varying intensity on the % level at ω_0 is present. This phenomenon is well-known from liquid crystalline systems with deuterated dopants.[35,36] There, the isotropic signal arises from molecules outside of the columns, which can undergo isotropic motions. In our case, obviously parts of the sample form smaller assemblies with less order and higher mobilities. Especially at the domain boundaries, one can easily envisage smaller amounts of less ordered material. The additional intensity seems to be highest in the spectra in the intermediate motional regime, because the main signal is then significantly reduced which makes the isotropic signal appear stronger. The isotropic signal decreases also on cooling the sample as compared to heating the sample. This is probably due to the formation of larger domains during the slow cooling process and thus to a smaller isotropic signal from domain boundaries.

The restricted mobility of the alkoxy side chains in the neighborhood of the core is probed with the sample **1e**, deuterated at the α-methylene position. For many discotic systems, it is well-known that the α-methylene units exhibit only small-angle librations in addition to the column rotation.[27,36,37] The temperature-dependent ^{2}H NMR spectra of **1e** (Figure 6) show even at −80 °C in the Cr_1 phase no rigid Pake patterns. The observed splitting is about 114 kHz and indicates small angle librations. At higher temperatures, the small angle librations increase. In the Cr_2 phase at 30 °C, the splitting is reduced further to 105 kHz. The transition to the LC phase is connected with a significant reduction of the quadrupole splitting. After cooling from the isotropic phase, the LC phase spectra of both the unoriented and the oriented sample exhibit a strong signal at ω_0 and two smaller peaks corresponding to a quadrupolar splitting of 18 kHz. Cooling from the LC phase to the crystalline phase yields again at 23 °C a Pake-like pattern. The phenomenon of a well-defined quadrupole splitting in the mesophase is known from triphenylene systems,[27,38] where the splitting δ of the α- C^2H_2 deuterons was found to depend on the temperature within the LC phase. This fact was taken as an indication for a change of the conformation of the alkyl chains

(33) Stallmach, U.; Schollmeyer, D.; Meier, H. *Chem. Mater.* **1999**, *11*, 2103.
(34) Wind, M.; Saalwächter, K.; Wiesler, U.-M.; Müllen, K.; Spiess, H. W. *Macromolecules* **2000**, *35*, 10071−10086.
(35) Kranig, W.; Boeffel, C.; Spiess, H. W. *Liq. Cryst.* **1990**, *8* (3), 375−388.
(36) Luz, Z.; Goldfarb, D.; Zimmermann, H. In *Nuclear Magnetic resonance of Liquid Crystals*; Emsley, J. W., Ed.; NATO ASI Series C; D. Reidel Publishing Company: Dordrecht, Netherlands, 1995; Vol. 141.
(37) Werth, M.; Leisen, J.; Boeffel, C.; Dong, R. Y.; Spiess, H. W. *J. Phys. II France* **1993**, *3*, 53−67.
(38) Goldfarb, D.; Luz, Z. *J. Chem. Phys.* **1983**, *78* (12), 7065.

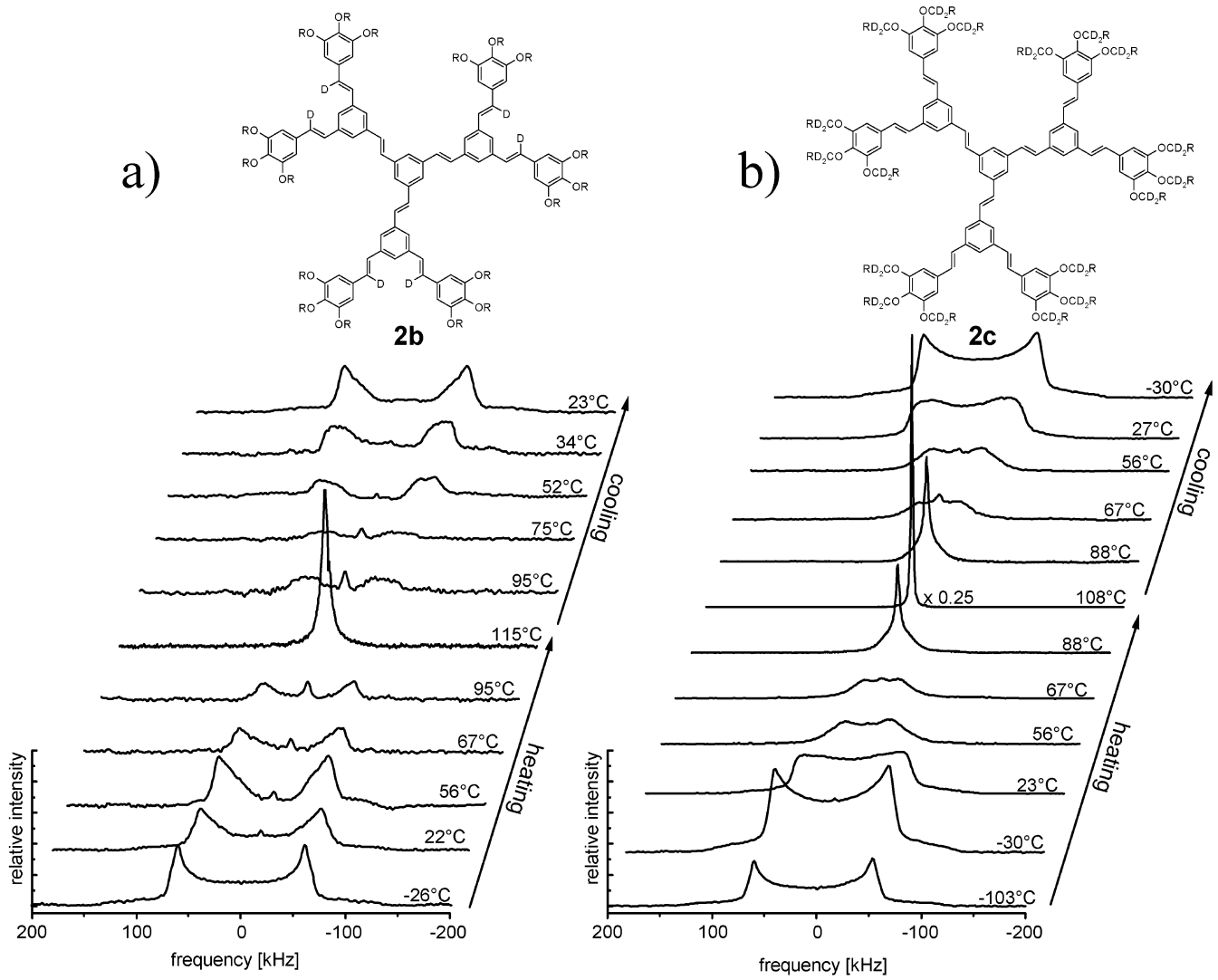

Figure 7. (a) Temperature-dependent ^{2}H NMR spectra of **2b**. (b) Temperature-dependent ^{2}H NMR spectra of **2c**. The intensity of the spectrum at 108 °C was scaled down by a factor of 0.25.

with temperature and could be analyzed in terms of the *gauche*−*trans* equilibrium at the α-carbon.[38] In our case, we do not observe a change in the splitting within the LC phase. A conformational analysis was also carried out for a discotic liquid crystal main chain polymer and the corresponding monomer/dimer and showed that the triphenylene monomer side chains are almost completely in *in-plane-trans* conformation (IPT); i.e., the O−CH_2 bond lies in the aromatic plane. For the polymer, a distribution between IPT (∼70%) and out-of-plane conformation (∼30%) was observed.[39] Such information could not be extracted from the data presented here, because the stilbenoid structure leads to an increased number of degrees of conformational freedom. Nonetheless, the strong sharp signal at the center of the spectrum and the two sharp signals with a quadrupole splitting of 18 kHz are consistent with preferred conformations of the α-methylene units of **1** in the LC phase. The α-methylene units carry out only weak, restricted librational motions in addition to the overall molecular dynamics, a behavior which is well-known from familiar systems.[27]

B. Second Generation Dendrimers 2. Having elucidated the molecular dynamics of the first generation dendrimer **1**, we now focus on the second generation dendrimer **2**. As will be shown in the following, the increase in size leads to significant changes in the molecular dynamics. Figure 7 illustrates the temperature-dependent ^{2}H NMR spectra of the second generation dendrimer deuterated at the outer olefinic position **2b** and at the α position of the aliphatic side chains **2c**. The temperature dependence of both series of spectra is quite similar, showing Pake-like shapes in the crystalline phase, broader spectra with a reduced quadrupolar splitting in the LC phases, and finally a single signal at ω_0 for the isotropic melt. The spectra of the side chain substituted **2c** are broader and exhibit reduced quadrupolar splittings at higher temperatures. This is an indication for additional librational motions of the α-methylene units. Apart from those librations, the dynamics of the two molecular segments seem to be alike.

The spectra of **2b** can be analyzed in more detail, yielding information about the motion of the outer stilbene units. In the crystalline phase, the spectra have Pake-like patterns with a quadrupole splitting of 127 kHz for **2b** at −26 °C. Therefore, the outer stilbene units are rigid on the fast time scale ($<10^{-4}$s) as it is expected for a solid phase. Upon heating, the quadrupole splitting is slightly reduced and the resonance broadens and loses intensity. Even at 95 °C in the Col_{ob} phase, the splitting of **2b**

(39) Hirschinger, J.; Kranig, W.; Spiess, H. W. *Colloid Polym. Sci.* **1991**, *269*, 993−1002.

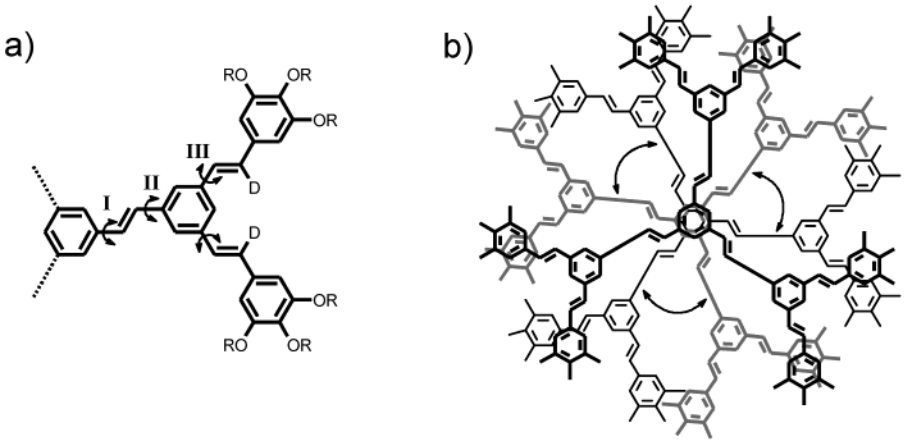

Figure 8. (a) Schematic drawing of a dendritic arm of **2** and the torsional freedom resulting from rotations around the three single bonds next to the olefins; dotted lines symbolize dendritic arms not shown here. (b) Schematic drawing of the second possible motional mechanism of **2**, which consists of jumps around the column axis.

is only reduced to 87 kHz. A fast rotation around the columnar axis, as found in the LC phase of **1**, would lead to a quadrupolar splitting at least reduced by a factor of 2. The observed small reduction of the quadrupolar splitting proves that **2** performs slower molecular motions in its LC phases and does not rotate like the first generation dendrimer **1**. Only in the isotropic phase the fast motional limit is reached. There, at 115 °C, solely an isotropic signal is observed. Upon cooling, the same spectra are obtained as on heating the sample. This indicates that no alignment of the outer aromatic rings in the magnetic field takes place. Nonetheless, an alignment of the columns cannot be completely excluded, since the outer aromatic rings can be twisted out of the plane of the core of the molecule to various degrees and thus adopt all sorts of orientations with respect to the external magnetic field. This torsional freedom around three different single bonds per dendritic arm (illustrated in Figure 8) makes it difficult, if not impossible, to figure out the mechanism of the molecular motion leading to the observed small reduction of the quadrupolar splitting. In principle, there are two possible mechanisms of molecular motion which might both be present in **2** and are depicted in Figure 8. First, the dendritic branches can rotate around the single bonds next to the olefins (Figure 8a). Second, jumps around the column axis can take place (Figure 8b). First generation dendrimers showed that single segments are mobile and twist out of the molecular plane up to an angle of 26° and only, on average, a planar shape may be formed necessary for aggregation and liquid crystal organization. Similar torsional freedom can be expected for the deuterated peripheral building blocks of second generation dendrimer **2**. Consequently, a single preferential angle between the C−D bonds and the column axis cannot be specified. Therefore, simulations determining jump angles and/or rates cannot be carried out in an unambiguous fashion. Nonetheless, it is clear from the small reduction of the quadrupolar splitting that the motions of **2** do not include any large angle motions or free rotations in the fast motional limit, since those kinds of motion would lead to a more efficient reduction of the quadrupole splittings. The intensity loss and the broadening of the spectra at higher temperatures indicate that the dynamics in **2** are on the intermediate time scale and below. Only the isotropic signal contributions at higher temperatures are due to moieties undergoing fast isotropic motions. The finding of slower dynamics in **2** as compared to **1** is strongly supported

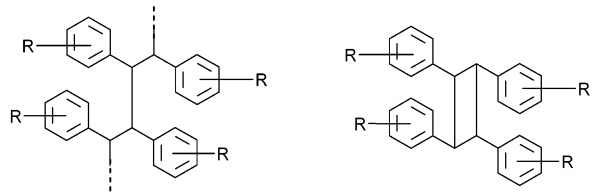

11 **12**

Figure 9. Photoproducts built by CC bond formation: methine structures **11** and cyclobutanes **12**.

by the fact that the spectra of **2c** (i.e., the sample deuterated at the α-methylene units) do not exhibit signals as sharp and intense as those of **1e**. Thus, even the dynamics of the α-methylene units are restricted to ill-defined intermediate motions. It should be noted that, apart from a broad foot, the spectra of **2c** at 88 °C are completely isotropic, although the phase transition to the isotropic phase is about 10 °C higher. Obviously, the melting of the alkyl chains precedes the isotropic melting of the complete mesogen.

Photoreaction within Different Phases. Previous studies by FTIR and UV−vis spectroscopy on spin-coated films (thickness of approximately 100−200 nm) of **1** and **2** at ambient temperature revealed an almost complete photodegradation of all olefinic double bonds.[7,14] The films were irradiated with a light of $\lambda = 350$ nm on the low energy side of the absorption maximum of **1** and **2** ($\lambda_{max} = 342$ nm), which is broadened and bathochromically shifted in the solid state compared to an absorption spectrum recorded for solutions in CH_2Cl_2 ($\lambda_{max} = 330$ nm). More detailed high-resolution ^{1}H NMR studies turned out to be difficult, since the signals of the products formed by statistical CC bond formation, i.e., protons of methine **11** or cyclobutane **12** structures (Figure 9), were partially covered by the CH_2O signals of the lateral chains. For more insight into how these reactions proceed in neat films, molecules **1e** and **2c** with deuterated α-methylene groups have been investigated. The deuteration in α-positions of lateral chains allows a detailed quantitative study of the progressing photoreactions by ^{1}H NMR spectroscopy. Figure 10 presents the ^{1}H NMR spectra of **1e** after exposure to a light of $\lambda = 350$ nm for 2 h in its different phases from the crystalline state to the isotropic liquid. Irradiation of the crystalline phase at room temperature does not result in any photoreaction, i.e., isomerizations or oligomerizations.

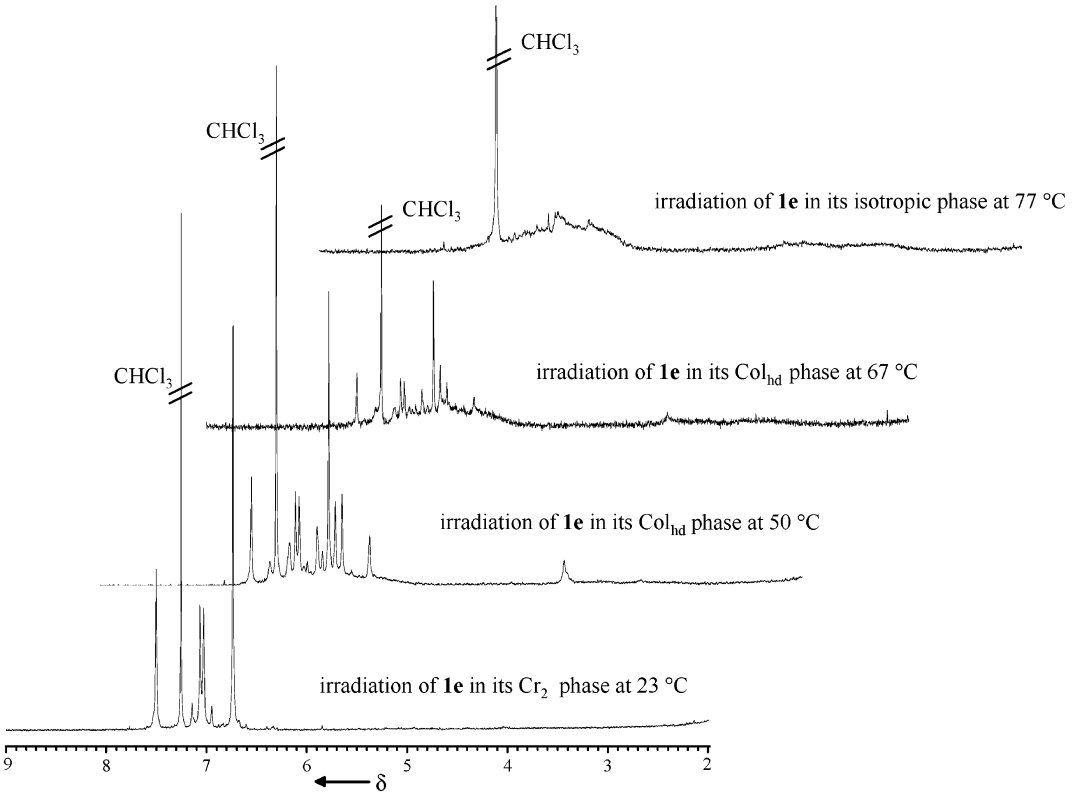

Figure 10. ^{1}H NMR spectra of dendrimer **1e** in $CDCl_3$, previously irradiated for 2 h with a light of $\lambda = 350$ nm in its different neat phases.

Obviously, the constraints of the crystal lattice prevent the stilbenoid molecules from phototransformations.[40] Photodegradation of double bonds begins when the material is heated to its liquid crystal phase. At the Cr/Col_{hd} transition, the mesogens start to rotate around their columnar axis and olefinic centers of neighboring molecules can approach each other within the average lifetime of the excited singlet state. The mean intracolumnar distances within the disordered hexagonal columnar phase is estimated to be 0.40 ± 0.01 nm.[41] Such distances are known to promote topochemically controlled photoreactions.[40] With the beginning conversion of double bonds at 50 °C, a dominant signal in the ^{1}H NMR spectrum at 4.37 ppm is observed, which appears also for cyclophane dimers of **1** formed via three cyclobutanes.[42] With irradiation of **1e** at higher temperatures, signals broaden and become a typical aspect of oligomer/polymer resonances. As the mobility of the molecules **1** in their neat phases increases, the conversion of double bonds increases too (Table 2). It is evident, that double bonds have to approach within the lifetime of the excited state, which was determined in solution for the parent compound, (*E*,*E*,*E*)-1,3,5-tristyrylbenzene, to be 8.3−13.6 ns.[43] The temperature-dependent increase of mobility in the range from $\tau_c = 10^{-5}$ s to $\tau_c \leq 10^{-7}$ s thus raises the probability of photoconversion. Interestingly, the photoreaction of olefinic centers is most efficient in the isotropic phase (Table 2). This observation accounts for aggregates remaining in the isotropic liquid.[44] Similarly, solution studies showed that, in apolar solvents where aggregates are preferentially formed, the photooligomerization is fast, whereas, at low concentration in good solvents, where almost no aggregation of molecules is expected, the reaction is slow.[5,7] Note that a conversion of double bonds of 49% in the isotropic phase for **1e** means that, on average, 1.5 olefin units per molecule have reacted. As soon as no monomer signal is present, all molecules are incorporated into the oligomers or polymers formed. MALDI-TOF analysis of a photoproduct after 5 h of irradiation at 50 °C (21% double bond conversion) shows signals for monomers, dimers, trimers, and tetramers (Figure 11). A signal at $m/z = 1298.1$ u demonstrates the presence of a cycloreversion product **13** (Figure 11), which can be formed only upon irradiation (N_2-Laser; 329 nm) of products with cyclobutane rings during the MALDI measurements. As already outlined earlier, photoconversion can lead to both cyclobutanes and methine structures. Unfortunately, it was not feasible to determine the portion of each structural unit in the photoproducts of stilbenoide dendrimers.

Table 2. Photochemical Conversion of Double Bonds by Irradiation of the Stilbenoid Dendrimers with a UV Light of $\lambda = 350$ nm in Their Different Phases

compound	phase	temperature [°C]	conversion of double bonds [%]
1e	Cr_2	23	0
1e	Col_{hd}	50	13
1e	Col_{hd}	67	16
1e	I	77	49
2c	Col_{hd}	23	7
2c	Col_{ob}	88	19
2c	I	108	38

(40) Ramamurthy, V.; Venkatesan, K. *Chem. Rev.* **1987**, *87*, 433−481.
(41) The intracolumnar distance of mesogens has been determined by evaluating the wide angle region of the powder X-ray pattern. Besides the halo at 0.44 nm attributed to the mean distance of the liquidlike aliphatic chains, the diffraction pattern of **1a** in the room temperature phase shows a broad reflection on the wide angle side of the halo, which indicates an intracolumnar distance of approximately 0.38 nm. In the LC phase at higher temperature, this reflection has disappeared and only the broad halo remains. From the asymmetry of the halo at wide angles, an intracolumnar distance of 0.40 ± 0.01 Å has been estimated.

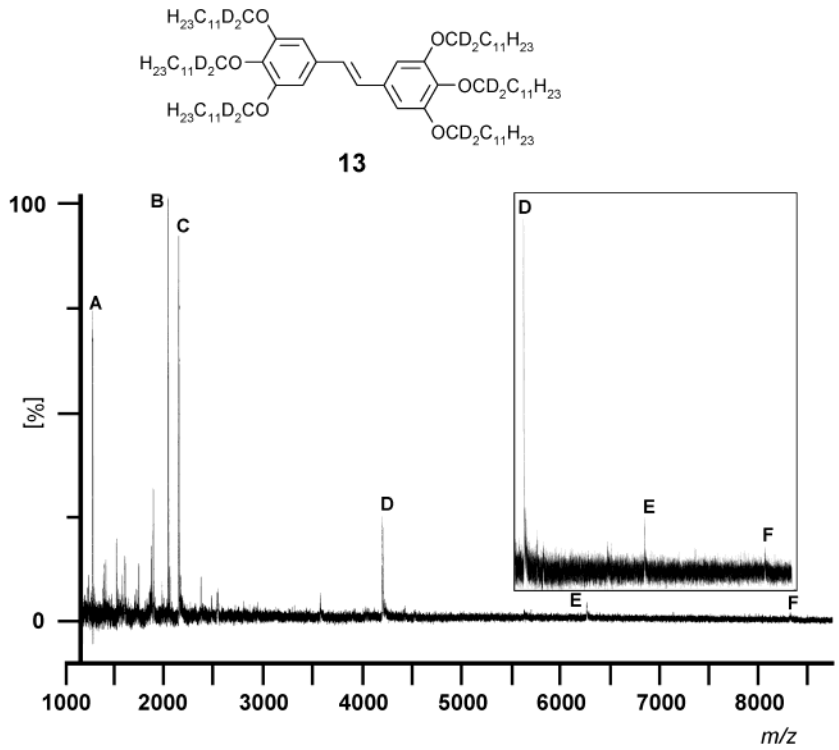

Figure 11. Cycloreversion product **13** formed during mass spectrometry (MALDI technique) of the photoproduct of **1e** and MALDI TOF spectrum of **1e** irradiated for 5 h with a light of $\lambda = 350$ nm, using dithranol doped with CF_3CO_2Ag as matrix and an N_2 laser ($\lambda_{ex} = 329$ nm). (A) $m/z = 1298.1$; M^+ (cycloreversion product **13**); (B) $m/z = 2060.8$; M^+ (monomer **1e**); (C) $m/z = 2169.8$; M^+ (monomer **1e** + Ag); (D) $m/z = 4231.5$; M^+ (dimer of **1e**); (E) $m/z = 6291.6$; M^+ (trimer of **1e**); (F) $m/z = 8354.9$; M^+ (tetramer of **1e**).

Analogous observations are made for the second generation dendrimer **2c** (Table 2). The photoconversion increases with temperature, thus, with larger mobility of the molecules. In contrast to **1**, photodegradation of olefinic centers is also observed at ambient temperature, since molecule **2** is in its low-temperature mesophase (Col_{hd}). In contrast to the crystal state of **1** at ambient temperature, dendrimer **2** is still mobile, which is demonstrated by the solid-state NMR studies. The photochemical conversion of the double bonds of compounds **1e** and **2c** in the respective mesophases and the isotropic phase after 2 h of irradiation is for both compounds in the same range. Although the latter show a higher viscosity and consequently a lower mobility of the stilbenoid molecules (only librational and small angle motions), the higher number of double bonds in a columnar segment compensates for the lower mobility during the photoreaction. Conversion of 38% in the isotropic phase of **2c** means that, on average, approximately three double bonds per molecule are photochemically transformed. Although the number of converted double bonds per molecule is higher for the second generation dendrimer, sharp monomer signals are still present. A prolonged irradiation (5 h) of **2c** leads to the complete disappearance of the long-wavelength absorption, which is characteristic for the stilbenoid chromophore.

Fluorescence Spectra in Different Phases. The results of the temperature-dependent emission measurements of dendrimers **1e** and **2a** are shown in Figure 12. Compared to the solution spectrum of **1** in $CHCl_3$ with a maximum at 426 nm, the fluorescence maximum of dendrimer **1e** is bathochromically shifted by 20 nm to 446 nm at ambient temperature in its crystal phase (Figure 12A). On heating, the peak maximum shifts hypsochromically until a value of 425 nm in the isotropic phase is reached. The shift to lower energy from solution to the crystalline state indicates an enhanced intermolecular interaction in the crystalline state; increase in temperature leads again to weaker interactions of molecules and, thus, to a shift to higher energies. More pronounced changes can be observed in the series of integrated peak intensities (Figure 12B). From a high value in the crystal phase, the integrated intensity decreases drastically at the transition to the LC phase. The value of the fluorescence peak integral diminishes continuously in the mesophase until the isotropic liquid is formed. In agreement with the results from ^2H NMR spectroscopy and photochemistry studies, the starting mobility of the molecules and the photoreaction quenches the fluorescence in the columnar disordered LC state. Thermally activated radiationless processes are decreasing the fluorescence intensity on increasing the temperature in the mesophase as it is generally expected.[45] On cooling the sample to ambient temperature, fluorescence intensity is not recovered at 25 °C, which is rationalized by the supercooling of the LC phase, already observed in DSC measurements and ^2H NMR spectroscopy.

The fluorescence maximum of the second generation dendrimer **2c** in its hexagonal phase is also bathochromically shifted to 446 nm compared to 428 nm in $CHCl_3$ solution. Similarly to **1e**, a hypsochromic shift to 429 nm is observed upon heating to the isotropic phase. However, a discontinuity at the phase transitions does not appear as can be seen in diagram D of Figure 12. There, a continuous decrease of the integrated intensity from

(42) Lehmann, M. Dissertation, Mainz, Germany, 1999.
(43) Meier, H.; Zertani, R.; Noller, K.; Oehlkrug, D.; Krabichler, G. *Chem. Ber.* **1986**, *119*, 1716.
(44) (a) Kleppinger, R.; Lillya, C. P.; Yang, C. *J. Am. Chem. Soc.* **1997**, *119*, 4097. (b) Lee, W. K.; Heiney, P. A.; Mccauley, J. P., Jr.; Smith, A. B., III. *Mol. Cryst. Liq. Cryst.* **1991**, *198*, 273.
(45) Levitsky, I. A.; Kishikawa, K.; Eichhorn, S. H.; Swager, T. M. *J. Am. Chem. Soc.* **2000**, *122*, 2474−2479.

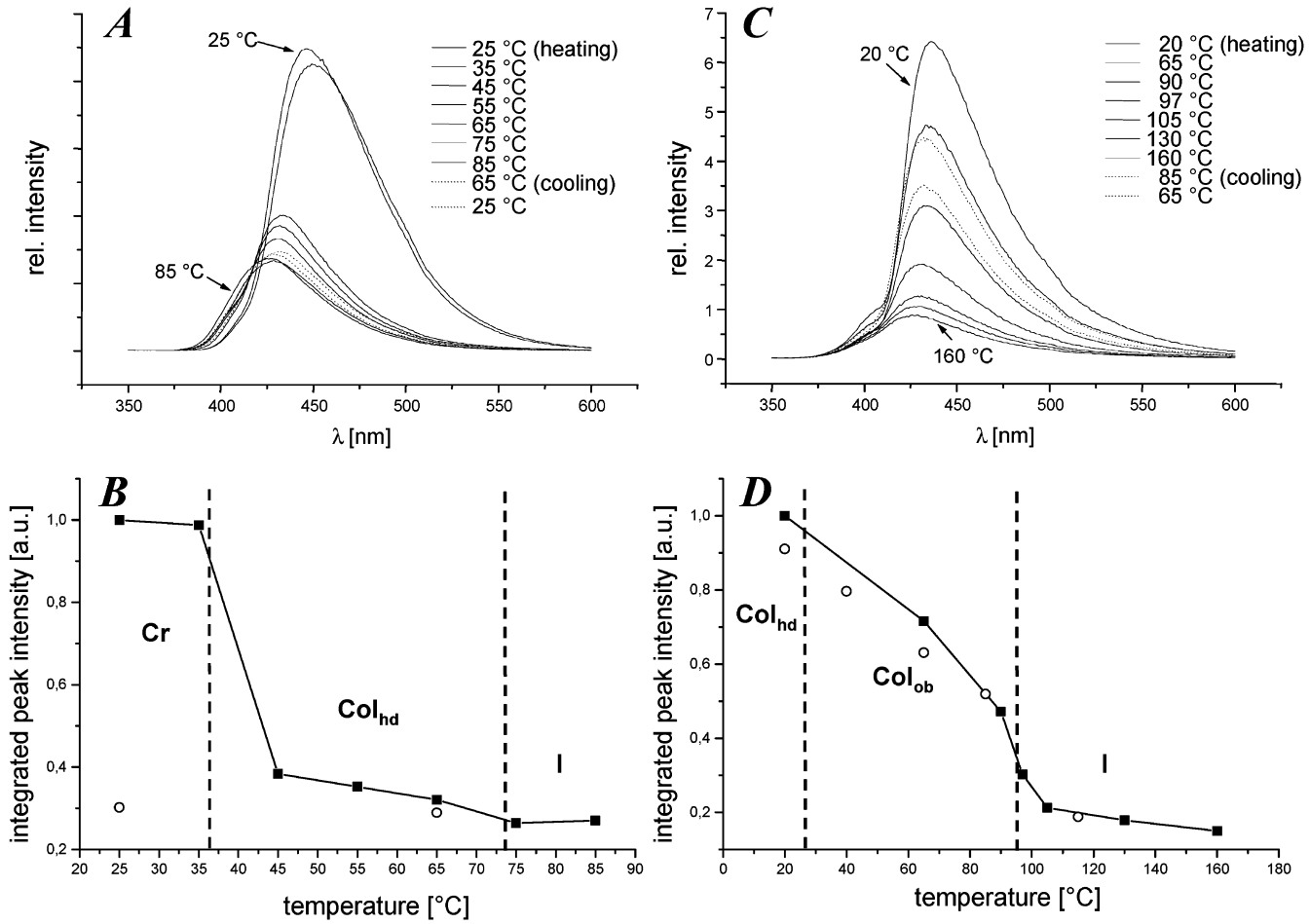

Figure 12. Temperature-dependent fluorescence of stilbenoid dendrimers **1e** and **2a** recorded between two CaF_2 plates with $\lambda_{ex} = 330$ nm. (A) Fluorescence spectra of **1e** at different temperatures. (B) Temperature-dependent integrated fluorescence intensity of **1e**: (■) heating, (○) cooling. (C) Fluorescence spectra of **2a** at different temperatures. (D) Temperature-dependent integrated fluorescence intensity of **2a**: (■) heating, (○) cooling.

the Col_{hd} over the Col_{ob} to the isotropic phase is observed. In the isotropic liquid, the integrated intensity decreases only slightly between 100 and 160 °C. The integral values are almost recovered upon cooling to ambient temperature (open circles). These findings can be rationalized by the increasing molecular mobility with increasing temperature. As demonstrated by the solid-state NMR experiments, mobility changes continuously; a sudden onset temperature for molecular motion as for **1e** at the Cr/Col_{hd} transition is not found, and consequently also no sharp decrease in the integrated fluorescence intensity is observed.

Summary and Conclusions

Temperature-dependent ^2H NMR in the neat phases of stilbenoid dendrimers shows the different molecular and segmental motions in their crystalline, liquid crystalline, and isotropic phases. A comprehensive study of the first generation dendrimer **1**, selectively deuterated in certain positions from the center to the periphery, reveals that molecules **1** perform an improper rotation around their columnar axis. Although **1** adopt an average planar shape which allows the regular aggregation of the mesogens in LC phases, styryl arms can deviate significantly from planarity due to the flat hypersurface of the potential energy when rotating a phenyl ring of a stilbene unit.[1] The latter deviation can be assigned to a dynamic equilibrium of various conformers. In contrast, dendrimers of the second generation do not show large angle motions. Only librations or small angle motions have been observed.

Molecular mobility turns out to be extremely important for the photochemical degradation of olefinic centers in neat phases. In the crystalline state of **1** where large amplitude mobility on a time scale below 10^{-4} seconds does not occur, no photoreaction has been detected, since olefinic units are not able to interact during the lifetime of the excited state of **1**. Instead enhanced emission of fluorescence light has been observed. When mesogens start to be mobile in the LC phases, fluorescence is quenched significantly and double bonds begin to transform via [2+2] cycloaddition or radical reactions.[1] When mobility increases, the probability that olefinic centers find each other during the lifetime of an electronic singlet state of one reaction site increases too. Consequently, in the isotropic phase in the vicinity of the phase transition, where a certain order within small aggregates can remain, the photoreaction is most efficient. Similar behavior is found for the second generation dendrimer **2**. However, since the molecules do not crystallize, no discontinuous transition is noticed. Interestingly, the conversion of double bonds is as fast as that for dendrimers **1**, although the molecular mobility is much lower. This is attributed to the larger number of double bonds within a columnar segment.

The presented work has correlated photochemistry and fluorescence in neat phases to the mobility of stilbenoid

dendrimers **1** and **2**. Molecular motion is a necessary condition for photooligomerization in these type of materials. For application in materials science, LC phases are highly interesting because of their self-organization and their self-healing effect. However, if mesogenic stilbenoid dendrimers are to be applied in electrooptical devices, such as light-emitting diodes[11] or photovoltaic cells,[12] precaution must be taken to avoid photochemical transformation. On the other hand, such photoreactions can be used for imaging techniques.

Acknowledgment. We are grateful to the Deutsche Forschungsgemeinschaft and the Fonds der Chemischen Industrie for financial support and to Ingo Schnell for carefully reading the manuscript and helpful discussion.

Supporting Information Available: Additional information as noted in the text. This material is available free of charge via the Internet at http://pubs.acs.org.

JA0366179